

SHORT COMMUNICATION

Resonance frequencies of honeybee (*Apis mellifera*) wingsChristopher J. Clark^{1,*}, Andrew M. Mountcastle^{2,3}, Emily Mistick¹ and Damian O. Elias⁴

ABSTRACT

During flight, insect wings bend and twist under the influence of aerodynamic and inertial forces. We tested whether wing resonance of honeybees (*Apis mellifera*) matches the wingbeat frequency, against the 'stiff element' hypothesis that the wing's first longitudinal mode exceeds the wingbeat frequency. Six bees were immobilized with their right wing pair outspread, and stimulated with a shaker while the normal modes were recorded with a scanning Doppler laser vibrometer. The lowest normal mode of the wings was the first longitudinal bending mode and, at 602 ± 145 Hz, was greater than the wingbeat frequency of 234 ± 13.9 Hz. Higher-order normal modes of the wing tended to incorporate nodal lines in the chordwise direction of the trailing edge, suggesting that their mode shape did not strongly resemble wing deformation during flapping flight. These results support the stiff element hypothesis for *Apis mellifera*.

KEY WORDS: Mode shape, Normal mode, Resilin

INTRODUCTION

Insect wings bend and twist over the course of the flight stroke, causing deformations by a combination of aerodynamic and inertial forces (Daniel and Combes, 2002). Because the wings are a periodically driven system, the resonance frequencies of the wings could be related to the wingbeat frequency at which they are driven. Here, we investigated the resonance spectrum of honeybee (*Apis mellifera*) wings to understand its potential effect on flight.

Driving a system near resonance can be beneficial because it is advantageous for energy transfer (i.e. little energy is lost to internal damping). The lowest resonance frequency of the wings will be the first longitudinal mode of the long axis (Fletcher, 1992). Flexion in this axis may be beneficial in certain scenarios. For example, it could increase stroke amplitude (as measured at the tip of the wing) relative to the excursion of this same angle as measured at the base of the wing, thereby mechanically amplifying the motion of the wing while permitting the muscles driving the wing to operate with lower strain. Thus, one possibility, the resonance hypothesis, holds that the wing resonances are matched to the wingbeat frequency. However, resonance can also be detrimental to flight, because driving a system at resonance potentially hinders control, especially the ability to modulate frequency away from the resonance frequency, which insects may need to maneuver. Moreover, the type of wing flexion that is known to have beneficial aerodynamic

effects is often perpendicular to the long axis of the wing, in the chordwise direction (Mistick et al., 2016; Mountcastle and Combes, 2013). The alternative stiff element hypothesis is that the resonance frequency of the first longitudinal mode of the wings is far above the wingbeat frequency. In this case, the wing acts as a stiff reactive element with respect to the fundamental wingbeat frequency. Our primary purpose was to test these two hypotheses.

We also explored a complication to the above hypotheses: harmonics. In insect flight, the wings do not oscillate in a perfect sinusoid, but rather include substantial rotation about the long axis (Dickinson et al., 1999). At least the first six integer harmonics of the wingbeat frequency play a meaningful role in describing the kinematics of flight (Arthur et al., 2014; Bae and Moon, 2008; Sueur et al., 2005). Thus, an insect flapping its wings at 200 Hz is mechanically exciting the wings at 200, 400, 600, 800, 1000 and 1200 Hz. Rigid bodies contain multiple resonance frequencies (normal modes) that are not integer multiples and vary in mode shape (Fletcher, 1992). Mode shape is the spatial distribution of relative motion (phase) across the object, in response to an ideal excitation. Although flat plates with uniform cross-sectional area and constant elastic modulus have easily predicted higher-order frequencies and mode shapes (Blevins, 1979), it is difficult to apply these models to insect wings, which do not have uniform cross-sectional area or elastic moduli.

It is intuitive to hypothesize that the lowest resonance frequency of the wings will be the first longitudinal mode. By contrast, it is harder to predict *a priori* the shape and frequency of higher modes – that is, whether higher-order modes incorporate torsional or chordwise motion that resemble wing deflections in flight. An alternative to modeling the resonance spectrum is to measure it empirically, as has been done for bird feathers (Clark et al., 2013) and insect wings. The lowest resonance frequency (first longitudinal mode) was investigated by Ha et al. (2013) for eight species of insect using a laser displacement sensor on a single point near the wingtip. However, their method did not allow them to examine higher normal modes. Moreover, they measured the resonance of excised wings, rather than *in situ*. Once removed from the animal, insect wings dry (lose mass) and stiffen (Mengesha et al., 2011), both of which should increase resonance frequency relative to the *in vivo* condition. Ha et al. (2013) measured either isolated forewings or hindwings (depending on species), but in most of the species, the forewing/hindwing pair is mechanically coupled during flight. Separating mechanically linked wings may alter the resonance frequency relative to the *in vivo* condition.

Scanning laser Doppler vibrometry (SLDV) allows mode shape analysis, where the mode shape of a given frequency is the spatial distribution of relative phase across the object. Here, we employed SLDV to observe higher-order modes of honeybee wings to see whether modes (1) corresponded to a harmonic of the wingbeat frequency, and (2) have a shape that resembled the chordwise deflection of the wing in flight. The resonance hypothesis would be supported if any normal modes matched both these criteria. If instead all resonance frequencies were well above the first six

¹Department of Evolution, Ecology and Organismal Biology, University of California, Riverside, CA 92521, USA. ²Department of Biology, Bates College, Lewiston, ME 04240, USA. ³Department of Organismic and Evolutionary Biology, Harvard University, Concord Field Station, Bedford, MA 01730, USA. ⁴Department of Environmental Science, Policy, and Management, University of California, Berkeley, CA 94720, USA.

*Author for correspondence (cclark@ucr.edu)

 C.J.C., 0000-0001-7943-9291

harmonics of the wingbeat frequency, the stiff element hypothesis would be supported.

MATERIALS AND METHODS

Fig. 1 shows our experimental setup. Six workers of *Apis mellifera* Linnaeus 1758 were caught on the University of California Berkeley campus on 8–12 January 2013. Each bee was filmed with a high-speed camera as it flew inside an insect enclosure to record its wingbeat frequency. Each bee was cold-anesthetized at 2°C for 10–15 min, then placed in a custom brace to immobilize the body and splay the wings out, similar to the brace pictured in Mountcastle and Combes (2014). The right forewing and hindwing were carefully arranged such that the hamuli along the anterior margin of the hindwing interlocked with the posterior margin of the forewing, recreating their relative positions during flight. A dab of cyanoacrylate was added to the base of the wings, to ensure their position remained fixed during the experiments. The glue also served to affix the hinge between the wing and the body at the base of the wing. Our pilot data showed that resonance frequencies of excised wings increased as the wings dried. Therefore, we collected *in vivo* measurements of resonance on the spread wings of immobilized bees that were alive ($n=4$) or had been dead for less than 30 min ($n=2$). We also compared the resonance spectrum of the ipsilateral forewing/hindwing pair first as a functional unit, then with the hindwing ablated, to determine whether and to what extent the hindwing modulated the resonant properties of the system.

Mechanical stimulation experiments with SLDV

Our general methods and equipment follow the mechanical stimulation experiments described in Clark et al. (2013) and are described here briefly, with the emphasis on slight methodological differences. The bee brace was affixed to a Brüel & Kjær mini-shaker (4810) with hot-melt adhesive, and stimulated with a frequency sweep from 0.003 to 10 kHz over the course of 0.320 s (3200 FFT lines). The SLDV (Polytec Inc.) sequentially scanned approximately 150 points across the wing (50 points in the ablation experiment), at a sampling rate of 51.2 kHz. The reference laser of the SLDV pointed at the base of the wing (Fig. 1). It measured the actual stimulus received by the base of the wing (e.g. Fig. 1A, right, middle), and allowed the SLDV to calculate the relative phase of

different points on the wing by comparing each point to a common reference. The coherence between the input voltage and the reference laser was computed. All scans had high coherence (i.e. >0.8) below 5 kHz, whereas coherence tended to decline above 5 kHz, indicating that our setup had reduced validity above 5 kHz. Average power spectra for all points across the wing were computed for the frequency range between 0 and 5 kHz.

Within the response power spectrum, amplitude maxima were interpreted to represent resonance frequencies (normal modes). We selected the six highest amplitude peaks within the response spectrum for further analysis, recorded their frequency, and thereafter conducted statistics according to the frequency of the peaks (ranked from lowest to highest: 1st=lowest frequency, 2nd=second lowest frequency, etc.). We generated amplitude-normalized animations of relative phase of these six resonance frequencies and examined by eye the mode shapes using the PSV software that runs the SLDV. We compared the lowest three resonance frequencies of both wings versus the forewing for the first six harmonics of the wingbeat.

Finally, using the SLDV, we also conducted a ‘fastscan’ of the wings. For fastscans, the test subject was scanned solely at the hovering wingbeat frequency previously recorded for that animal. This technique eliminates any effect of a time-varying frequency sweep input, as the shaker drives the object at a single frequency. The purpose of this test is to rapidly confirm trends suggested by the full scan.

RESULTS AND DISCUSSION

The lowest resonance frequency (normal mode) of all bee wings was the first longitudinal bending mode, which was 602 ± 145 Hz ($n=6$). Little to no chordwise motion was apparent in this mode. All higher-order normal modes contained chordwise nodal lines that generally extended from the trailing edge of the wing partway toward the wing center, but usually not extending all the way to the leading edge. The second normal mode (1.10 ± 0.25 kHz, $n=6$) showed either one nodal line ($N=3$) or two nodal lines ($N=3$) (compare arrows in Fig. 2C versus Fig. 2D). The angle of this nodal line varied from chordwise (Fig. 2A2) to spanwise (Fig. 2B2), and was most often somewhere between the two, at an angle perpendicular to the distal trailing edge of the wing (Fig. 2). For subsequent normal modes

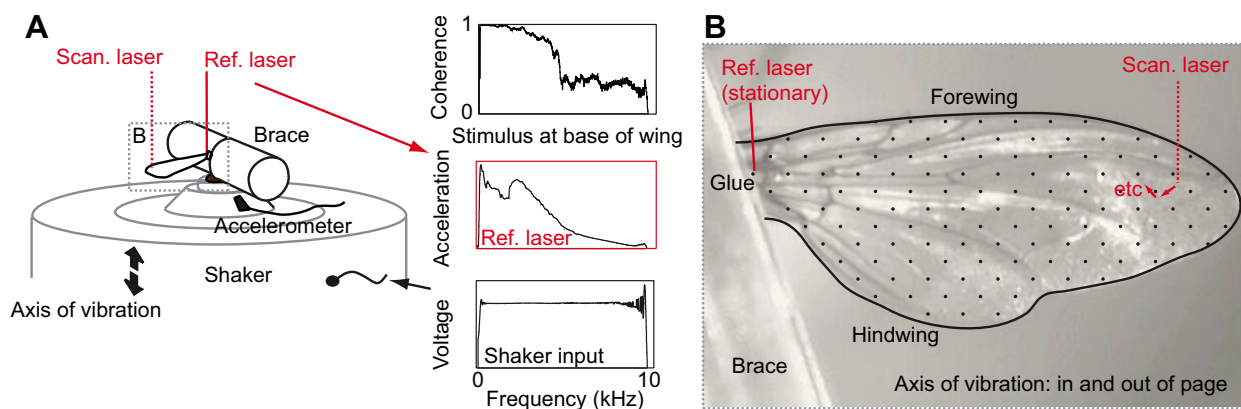


Fig. 1. The experimental setup. (A) Bees were sequestered alive inside a cylindrical brace (left). This brace was affixed to a shaker, which was driven by the scanning laser Doppler vibrometry (SLDV) controller. The input voltage from the controller was approximately constant between 0 and 10 kHz (right, bottom), producing an acceleration profile that was nearly flat (as verified by an accelerometer; data not shown). The scanning laser Doppler vibrometer comprised two lasers: the scanning (scan.) laser and the reference (ref.) laser. The reference laser was stationary and focused on the base of the wing, thus measuring the acceleration stimulus as experienced by the wing (right, middle). The coherence (right, top) between the input (right, bottom) and the scanning laser was near 1 below 5 kHz, but declined at higher frequencies. (B) Photo of a wing from the SLDV camera (see boxed region in A, left). The dots represent the approximate sampling scheme of the scanning laser, which scanned points sequentially. The hinge at the base of the wing was fixed in place with glue.

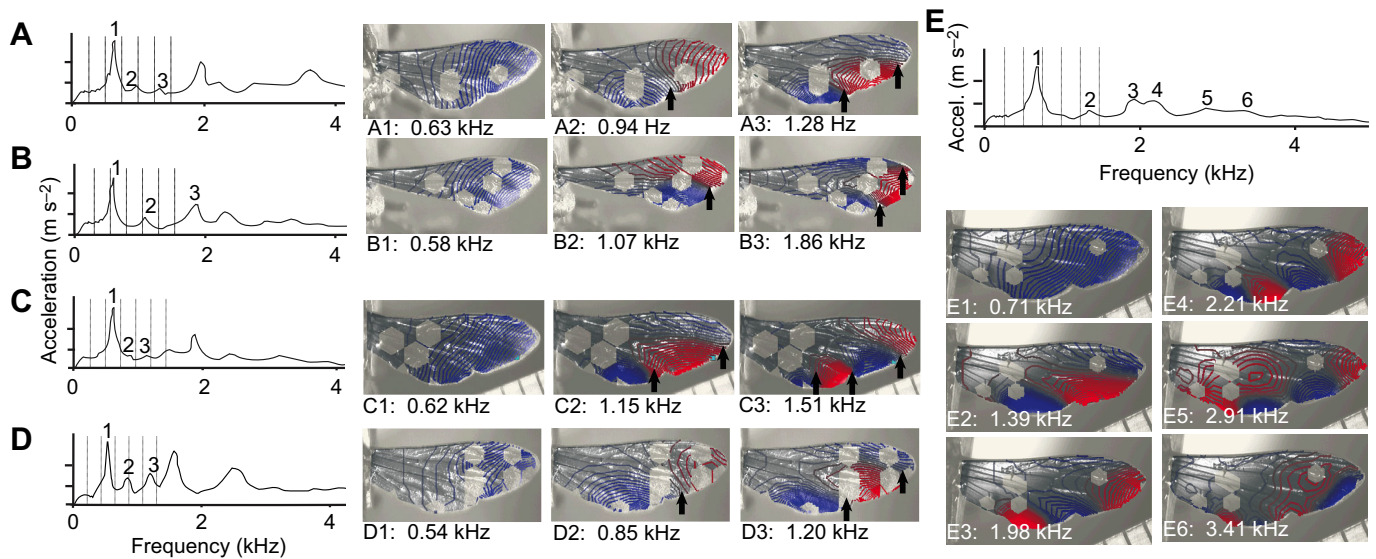


Fig. 2. Frequency response and mode shape of four *Apis mellifera* wings in response to mechanical stimulation from a shaker. Colored isolines indicate amplitude, and red versus blue indicates opposite phase. Arrows point to nodal lines that separate regions of opposite phase. Points with missing data appear as hexagons within the isolines. (A,B) Effects of hindwing removal (A, before; B, after): mode shape is not substantially affected by ablation of the hindwing. (C,D) Variation in mode shape of two more individuals, where the individual in D has an additional node for the second (C2 versus D2) and third (C3 versus D3) peak resonance frequencies. (E) The six first peak resonance frequencies for a fourth *A. mellifera* individual, showing an increase in the number of nodes with increasing peak frequency.

3–6, nodal lines did not change in angle but increased in number with each succeeding peak (frequency 3: 1.61 ± 0.36 kHz, frequency 4: 2.50 ± 0.99 kHz, frequency 5: 3.18 ± 0.88 kHz, frequency 6: 3.76 ± 0.71 kHz; $N=6$; Fig. 2; intact wings). At higher fundamental frequencies, the nodal pattern/mode shape became increasingly complex (Fig. 2E).

In support of the stiff element hypothesis, the first fundamental frequency (602 ± 145 Hz) was substantially higher than the wingbeat frequency of our individual bees (234 ± 13.9 Hz; paired *t*-test, $P=9.2 \times 10^{-8}$, $n=6$; Fig. 3). The resonance spectrum of the wing at

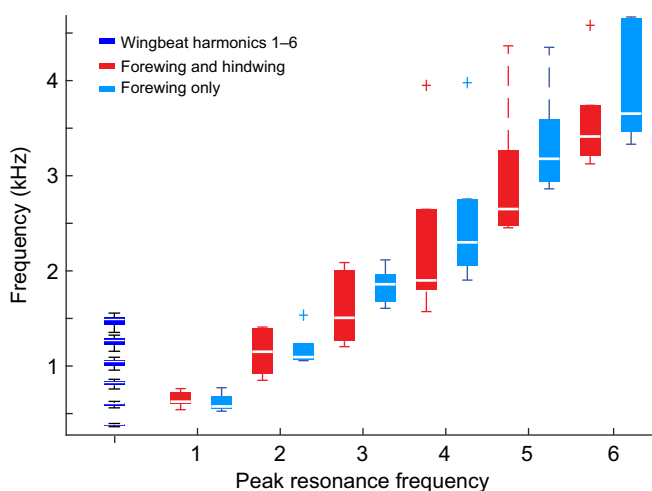


Fig. 3. First six harmonics of wingbeat frequency and first six normal modes of honeybee wings with and without hindwing. The first six harmonics of wingbeat frequency do not correspond directly to individual resonance frequencies. Ablating the hindwing (blue) did not result in a significant change in frequency relative to the same intact individuals (red) (two-tailed paired *t*-tests, frequencies 1–6, respectively: $P=0.06$, $P=0.81$, $P=0.12$, $P=0.11$, $P=0.06$, $P=0.24$; $n=5$). Box and whisker plots show median, quartile and range of data points, with outliers plotted as crosses.

the wingbeat frequency (rather than at a peak in the spectrum) revealed that the mode shape at this frequency contained little flexion, supporting the stiff element hypothesis, and this pattern was confirmed in the fastscan analyses (data not shown). Removing the hindwing did not result in a consistent change in resonance frequency in any of the first three fundamental frequencies (frequency 1–3: $P=0.064$, $P=0.81$, $P=0.12$, paired *t*-tests, $n=6$; Fig. 3). Because of the mechanical linkage between the forewing and hindwing, we had expected the hindwing to affect resonance frequencies that exhibited chordwise deflection. Our contrary finding suggests that hindwing coupling with the forewing is flexible or loose. It is possible that our manual arrangement of the forewing/hindwing overlap in this experiment did not completely recreate the extent to which these wings are mechanically interlocked *in vivo*. Moreover, our preparation included gluing the hinge at the base of the wing (Fig. 1B). Addition of this small amount of glue likely increased rigidity and the frequency of the first longitudinal mode. We suggest higher-order modes (Fig. 2) should be unaffected by this glue as, in our experience, pinning boundary conditions affect lower-order modes more so than higher-order modes, e.g. in hummingbird feathers (Clark et al., 2013).

The mean value of the third normal mode of the wings was well above the sixth harmonic of the wingbeat, and so is unlikely to be excited by the wingbeat. The second resonance frequency, by contrast, had an average of 1.10 ± 0.25 kHz, a range that spans the fourth, fifth and sixth harmonics of the wingbeat frequency (936, 1170, 1404 Hz, respectively). This resonant mode included substantial chordwise motion along one or two nodal lines, and so is the likeliest candidate for a match between a wing resonance frequency and a component of motion of the wings during flapping. Thus, it is plausible that the wing is tuned to this frequency, in order to minimize damping and maximize its elastic response to being flapped. However, this possibility is tempered by two observations. First, an alternative explanation for the pattern we have uncovered is that all stiff, flat objects must have various resonance frequencies,

and the wingbeat frequency has many integer multiples, so perhaps it was inevitable that a resonance frequency aligned with a wingbeat frequency harmonic. A better test of the resonance hypothesis would be to examine whether the mode shape of the second normal mode resembled the operating deflection shape of the 4th, 5th or 6th harmonic of the bee wing's motion, as was done with feathers in a comparison of mode of flutter of feathers versus their resonance frequency (Clark et al., 2013). We have no such data to present here: attempts to use laser vibrometry to measure wing stroke kinematics of insects (e.g. mosquitoes) failed (C.J.C. and A.M.M., unpublished) because the amplitude of insect wing motion (particularly rotation) is too high. Second, we only measured one species of insect. If multiple species of insect showed the same pattern despite differences in wing size, shape or wingbeat frequency, it would bolster the argument that wing resonance has evolved in response to a harmonic of the wingbeat frequency. Until these alternatives are explored further, we suggest that the simplest interpretation of our data is support for the stiff element hypothesis.

This conclusion is in general agreement with the conclusion of Ha et al. (2013), that the fundamental frequency of the wings is significantly different from the wingbeat frequency. Ha et al. (2013) found fundamental frequency (lowest mode) exceeded wingbeat frequency for all insect groups tested except Hymenoptera, while we found the lowest mode exceeded wingbeat frequency for *A. mellifera* (Hymenoptera). Ha et al. (2013) measured the first longitudinal mode for the wings of several species of insect, but on excised wings, which are stiffer than *in vivo* wings (Mengesha et al., 2011). Our preliminary trials of excised wings suggested that once the wings had dried, resonance frequencies of this mode increased by 32% (from 340 Hz to 450 Hz), 75 min after wing removal from the animal ($n=1$), which is why we conducted our primary experiment on wings attached to the animal. This effect potentially biases the data presented by Ha et al. (2013) toward higher natural frequencies than would be found *in vivo*. Adjusting Ha et al.'s (2013) data downward by 32% would cause their results for hymenoptera and ours to be even more disparate. In the species they measured, where natural frequency was higher than wingbeat frequency, their conclusion would not change, but it would reduce the difference between natural frequency and

wingbeat frequency. It seems likely that the effects of drying may be species specific. We suggest that future studies of this topic should, if feasible, leave the wings attached to the insect when measuring their resonance, as this is the natural condition.

Competing interests

The authors declare no competing or financial interests.

Author contributions

Conceptualization: C.J.C., A.M.M.; Methodology: C.J.C., A.M.M., D.O.E.; Formal analysis: E.M.; Writing - original draft: C.J.C., E.M.; Writing - review & editing: C.J.C., A.M.M., E.M., D.O.E.; Supervision: C.J.C.

Funding

This work was supported by the National Science Foundation (IOS-0920353).

References

- Arthur, B. J., Emr, K. S., Wytenbach, R. A. and Hoy, R. R. (2014). Mosquito (*Aedes aegypti*) flight tones: Frequency, harmonicity, spherical spreading, and phase relationships. *J. Acoust. Soc. Am.* **135**, 933–941.
- Bae, Y. and Moon, Y. J. (2008). Aerodynamic sound generation of flapping wing. *J. Acoust. Soc. Am.* **124**, 72–81.
- Blevins, R. D. (1979). *Formulas for Natural Frequency and Mode Shape*. New York: Van Nostrand Reinhold Company.
- Clark, C. J., Elias, D. O., Girard, M. B. and Prum, R. O. (2013). Structural resonance and mode of flutter of hummingbird tail feathers. *J. Exp. Biol.* **216**, 3404–3413.
- Daniel, T. L. and Combes, S. A. (2002). Flexible wings and fins: bending by inertial or fluid-dynamic forces? *Integr. Comp. Biol.* **42**, 1044–1049.
- Dickinson, M. H., Lehmann, F.-O. and Sane, S. P. (1999). Wing rotation and the aerodynamic basis of insect flight. *Science* **284**, 1954–1960.
- Fletcher, N. H. (1992). *Acoustic Systems in Biology*. New York: Oxford University Press.
- Ha, N. S., Truong, Q. T., Goo, N. S. and Park, H. C. (2013). Relationship between wingbeat frequency and resonant frequency of the wing in insects. *Bioinspir. Biomim.* **8**, 046008.
- Mengesha, T. E., Vallance, R. R. and Mittal, R. (2011). Stiffness of desiccating insect wings. *Bioinspir. Biomim.* **6**, 014001.
- Mistick, E. A., Mountcastle, A. M. and Combes, S. A. (2016). Wing flexibility improves bumblebee flight stability. *J. Exp. Biol.* **219**, 3384–3390.
- Mountcastle, A. M. and Combes, S. A. (2013). Wing flexibility enhances load-lifting capacity in bumblebees. *Proc. R. Soc. Biol. Sci. Ser. B* **280**, 20130531.
- Mountcastle, A. M. and Combes, S. A. (2014). Biomechanical strategies for mitigating collision damage in insect wings: structural design versus embedded elastic materials. *J. Exp. Biol.* **217**, 1108–1115.
- Sueur, J., Tuck, E. J. and Robert, D. (2005). Sound radiation around a flying fly. *J. Acoust. Soc. Am.* **118**, 530–538.